



# Physical, Thermal, and Spectroscopic Characterization of the Biofield Energy Treated Pyridoxine Hydrochloride

Mahendra Kumar Trivedi<sup>1</sup> and Snehasis Jana<sup>2\*</sup>

<sup>1</sup>Trivedi Global, Inc., Henderson, Nevada, USA

<sup>2</sup>Trivedi Science Research Laboratory Pvt. Ltd., Thane (W), India

**\*Corresponding author:** Snehasis Jana, Trivedi Science Research Laboratory Pvt. Ltd, Thane (W), India, Tel: +91-022-25811234;

Email: publication@trivedieffect.com

**Received Date:** March 05, 2020; **Published Date:** April 03, 2020

## Abstract

Pyridoxine hydrochloride is an important cofactor for the regulation of various enzymatic activities and used in the treatment of vitamin B<sub>6</sub> deficiency and associated diseases. This study was aimed to analyse the impact of the Trivedi Effect®-Energy of Consciousness Treatment on the physicochemical, spectral, and thermal properties of pyridoxine hydrochloride. The pyridoxine sample was equally divided into control/ untreated and the Biofield Energy Treated pyridoxine. The treated pyridoxine sample received the Biofield Energy Treatment (the Trivedi Effect®) remotely for ~3 minutes by Mr. Mahendra Kumar Trivedi, who was located in the USA, while the test samples were located in the research laboratory in India. The treated sample was designated as the Biofield Energy Treated sample. The analysis revealed that the particle size values at d<sub>10</sub>, d<sub>50</sub>, d<sub>90</sub>, and D(4,3) in the Biofield Energy Treated sample were significantly altered by -5.97%, -0.70%, 20.26%, and 14.15%, respectively compared to the control sample. Subsequently, the specific surface area of the treated sample was significantly increased by 3.22% than the control sample. Besides, the PXRD analysis showed that the relative intensities as well as the crystallite sizes of various characteristic peaks in the treated sample were significantly altered from -7.50% to -41.32% and -38.48% to 9.10%, respectively compared with the control sample.

Also, the treated sample showed a significant reduction of 6.23% in the average crystallite size compared with the control sample. The thermal analysis involving the TGA study revealed the significant reduction in the weight loss in 1st and 3rd steps of degradation of the treated sample by 19.05 and 3.03%, respectively along with 1.02% decrease in the total weight loss compared with the control sample. Thus, the thermal stability of the treated sample was observed to be increased compared to the control sample. The DSC analysis showed a slight reduction in the melting point of the treated sample, however, the latent heat of fusion was increased by 15.65% compared with the control sample. Thus, the Trivedi Effect® might help in producing a novel polymorphic form of pyridoxine hydrochloride, which may show improved solubility, dissolution rate, and bioavailability compared with the untreated sample. This Biofield Energy Treated pyridoxine hydrochloride might be beneficial in designing a better pharmaceutical and nutraceutical formulation in terms of better therapeutic responses against vitamin B<sub>6</sub> deficiency, with microcytic anemia, autoimmune disorders, Crohn's disease, ulcerative colitis, glossitis, dermatitis with cheilosis, pyridoxine-dependency seizures, electroencephalographic abnormalities, metabolic disorders, celiac disease, pulmonary tuberculosis, hyperhomocysteinemia, dysmenorrhea, etc.

**Keywords:** Pyridoxine Hydrochloride; The Trivedi Effect®; Energy of Consciousness Treatment; PXRD; PSA; DSC; TGA

**Abbreviations:** PLP: Pyridoxal Phosphate; RDA: Recommended Dietary Allowance; PSA: Particle Size Analysis; TGA: Thermogravimetric Analysis; DSC: Differential Scanning Calorimetry; PXRD: Powder X-ray Diffraction; FT-IR: Fourier Transform Infrared; TGA: Thermal Gravimetric Analysis; DTG: Differential Thermogravimetric Analysis; PSA: Particle Size Analysis; PXRD: Powder X-ray Diffraction; ADHD: Attention Deficit Hyperactivity Disorder.

## Introduction

Pyridoxine Hydrochloride is considered as an important cofactor for the regulation of various enzymatic activities in more than 100 enzyme reactions, such as synthesis of neurotransmitters, amino acids (protein metabolism), and sphingolipids. It is the hydrochloride salt of pyridoxine, a water-soluble vitamin B. Its active form, pyridoxal 5'-phosphate (PLP) play a vital role in the body, and it defined as a very essential vitamin for the function of nervous system, immune systems, red blood cells, and to maintain normal blood sugar level. Vitamers has been defined due to its six compounds generic name with vitamin B<sub>6</sub> activity viz. pyridoxine (an alcohol), pyridoxal (an aldehyde), and pyridoxamine (an amino group) with their respective 5'-phosphate esters [1,2]. Vitamin B<sub>6</sub> also plays a major role in cognitive development through biosynthesis of neurotransmitters and also in sustaining the normal levels of homocysteine, an amino acid in the blood. In addition, it is majorly involved in gluconeogenesis, glycogenolysis, immune function (such as promoting lymphocytes and cytokines production), and hemoglobin formation. Recommended Dietary Allowance (RDA) has been defined as the requirements such as age, sex, nutrient requirements in pregnancy and lactation (~2 mg) [3]. It is naturally present among various foods and readily available as a dietary supplement. Some major sources such as fish, beef liver and other organ meats, potatoes, and other starchy vegetables, and fruit (non-citrus) are the richest source of vitamin B<sub>6</sub>, while fortified cereals, beef, poultry, starchy vegetables, and some non-citrus fruits are the major dietary foods in the United States for dietary vitamin B<sub>6</sub> [4,5]. Besides, 28-36% of the population use vitamin supplements as the source of vitamin B and its other complex. This is available as oral capsules or tablets or in liquids, and its absorption is almost similar to that of fortified foods and vegetables. The deficiency of vitamin B<sub>6</sub> is associated with microcytic anemia, electroencephalographic abnormalities, autoimmune disorders, celiac disease, Crohn's disease, ulcerative colitis, impaired renal function, dermatitis with cheilosis, and glossitis (swollen tongue), depression and confusion, along with the weakened immune function [6]. In addition, its deficiency also leads to abnormally acute hearing, irritability, and convulsive seizures [7]. Vitamin B<sub>6</sub> rich diet would help to reduce the clinical symptoms of rheumatoid arthritis [8]

cardiovascular diseases, cancer, cognitive function, and also reduce the premenstrual syndrome [9,10]. Nowadays, the Biofield Energy Treatment is considered as a novel approach that is observed to be useful in improving the absorption as well as the bioavailability of the compound [11-13]. The Biofield Energy is considered as an ancient healing practice, which is based on the transmission of life force energy by the Biofield Energy practitioner.

The Biofield Energy is a dynamic low-level electromagnetic field, which is infinite and para-dimensional and present surrounds the human body [14,15]. Thus, a human has the ability to harness energy from the universe and can transmit it to any living organism(s) or non-living object(s) around the globe. The object or recipient always receives energy and responds in a useful way. This process is known as the Trivedi Effect® - Biofield Energy Treatment [16,17]. The Biofield Energy Treatment has been significantly reported to affect the physicochemical properties of various nutraceuticals [18-20], pharmaceuticals [21-23], organic compounds [24-26], metals and ceramic [27,28], impacting the efficacy in different living cells [29,30], and improving the productivity of agricultural crops [31,32]. Thus, this study was designed to analyse the effect of the Biofield Energy Treatment (the Trivedi Effect®) on the physicochemical, spectral and thermal properties of pyridoxine hydrochloride by using the analytical techniques such as particle size analysis (PSA), powder X-ray diffraction (PXRD), FT-IR and UV-visible spectroscopy, thermogravimetric analysis (TGA), and differential scanning calorimetry (DSC).

## Materials and Methods

### Chemicals and Reagents

Pyridoxine hydrochloride was purchased from Tokyo Chemical Industry Co. Ltd., Japan. All other chemicals used in the experiment were of analytical grade available in India.

### Consciousness Energy Healing Treatment Strategies

The pyridoxine hydrochloride sample was divided into two parts. One part of the pyridoxine was considered as control/untreated sample, which was not received the Biofield Energy Treatment. The second part of the pyridoxine sample was received the Trivedi Effect®-Consciousness Energy Treatment remotely under standard laboratory conditions for ~3 minutes by Mr. Mahendra Kumar Trivedi and termed as the Biofield Energy Treated/the Trivedi Effect® Treated pyridoxine. Mr Trivedi was located in the USA, while the test samples were located in the research laboratory in India. This Biofield Energy Treatment was provided through the Mahendra Trivedi's unique energy transmission process to the test item. Consequently, the Control sample was subjected to a "sham" healer (who did not have any knowledge about

the Biofield Energy Treatment) under the similar laboratory conditions. The control as well as the Biofield Energy Treated pyridoxine hydrochloride samples were kept in similar sealed conditions and further characterized by using PSA, PXRD, FT-IR, UV-Vis, TGA/DTG, and DSC.

## Characterization

### Particle size analysis (PSA)

The particle size analysis was done using the wet method, which involves the use of the instrument, Malvern Mastersizer 3000 (UK). The instrument has a detection range between 0.01  $\mu\text{m}$  to 3000  $\mu\text{m}$  [33], and the method involves the filling of sample unit (Hydro MV) with light liquid paraffin oil, which acts as dispersant medium. The refractive index values for dispersant medium and samples were 0.0 and 1.47, respectively. Later on, it was stirred at 2500 rpm, and the measurement was taken twice after reaching obscuration in between 10% and 20%, followed by averaging both measurements. The PS analysis provides data in the form of  $d_{10}$   $\mu\text{m}$ ,  $d_{50}$   $\mu\text{m}$ ,  $d_{90}$   $\mu\text{m}$ , and D(4,3) values, representing the particle diameter corresponding to 10% 50% and 90% of the cumulative distribution. The calculations were done by using software Mastersizer V3.50.

The percent change in particle size (d) for  $d_{10}$ ,  $d_{50}$ ,  $d_{90}$  and D(4,3) was calculated. using following equation 1:

$$\% \text{ change in particle size} = \frac{[d_{\text{Treated}} - d_{\text{Control}}]}{d_{\text{Control}}} \times 100 \quad (1)$$

Where,  $d_{\text{Control}}$  and  $d_{\text{Treated}}$  are the particle size ( $\mu\text{m}$ ) for at below 10% level ( $d_{10}$ ), 50% level ( $d_{50}$ ), and 90% level ( $d_{90}$ ) of the control and the Biofield Energy Treated samples, respectively. Percent change in surface area (S) was calculated using following equation 2:

$$\% \text{ change in particle size} = \frac{[d_{\text{Treated}} - d_{\text{Control}}]}{d_{\text{Control}}} \times 100 \quad (2)$$

Where,  $S_{\text{Control}}$  and  $S_{\text{Treated}}$  are the surface area of the control and the Biofield Energy treated pyridoxine hydrochloride, respectively.

**Powder X-ray diffraction (PXRD) analysis:** The PXRD analysis of the control and the Biofield Energy Treated samples of pyridoxine hydrochloride was done with the help of PANalytical X'Pert3 powder X-ray diffractometer, UK. In this, the copper line was used as the radiation source for diffracting the analyte at 0.154 nm X-ray wavelength, which is running at 40 mA current and 45 kV voltage. Also, the scanning rate for instrument was kept at 18.87°/second over a 2 $\theta$  range of 3-90° and the ratio of  $K\alpha$ -2 and  $K\alpha$ -1 was 0.5 (k, equipment constant). The data produced by the instrument

was collected with the help of X'Pert data collector and X'Pert high score plus processing software. It provides the data in the form of a chart of the Bragg angle (2 $\theta$ ) vs. intensity (counts per second), and a table providing information regarding the peak intensity counts, d value ( $\text{\AA}$ ), full width half maximum (FWHM) ( $^{\circ}2\theta$ ), relative intensity (%), and area (cts $^{\circ}2\theta$ ). From this data, the crystallite size (G) was analyzed with the help of the Scherrer equation (3) as follows:

$$G = k\lambda / (b\text{Cos}\theta) \quad (3)$$

Where, k is the equipment constant (0.5),  $\lambda$  is the X-ray wavelength (0.154 nm); b in radians is the full-width at half of the peaks and  $\theta$  is the corresponding Bragg angle.

Later on, the percent change in crystallite size (G) of pyridoxine hydrochloride was calculated using following equation 4:

$$\% \text{ change in crystallite size} = \frac{[G_{\text{Treated}} - G_{\text{Control}}]}{G_{\text{Control}}} \times 100 \quad (4)$$

Where,  $G_{\text{Control}}$  and  $G_{\text{Treated}}$  are the crystallite size of the control and the Biofield Energy Treated pyridoxine hydrochloride samples, respectively.

**Fourier transform infrared (FT-IR) spectroscopy:** FT-IR spectroscopy of pyridoxine hydrochloride was done by using Spectrum ES Fourier transform infrared spectrometer (Perkin Elmer, USA) with the frequency array of 400-4000  $\text{cm}^{-1}$ . The process involves pressed KBr disk technique in which, ~2 mg of sample was taken along with about 300 mg of KBr as the diluent, followed by forming the pressed disk and running the sample in the spectrometer.

**Ultraviolet-visible spectroscopy (UV-Vis) analysis:** The UV-Vis spectral analysis of the control and the Biofield Energy Treated pyridoxine hydrochloride samples was done with the help of Shimadzu UV-2400PC SERIES with UV Probe (Shimadzu, JAPAN). The spectrum was recorded in the wavelength range of 190-800 nm using 1 cm quartz cell having a slit width of 0.5 nm. The absorbance spectra (in the range of 0.2 to 0.9) and wavelength of maximum absorbance ( $\lambda_{\text{max}}$ ) were recorded.

**Thermal gravimetric analysis (TGA) / Differential thermogravimetric analysis (DTG):** TGA/DTG analysis was done using TGA Q500 thermoanalyzer apparatus, USA under dynamic nitrogen atmosphere (50 mL/min). It involves heating the samples from 25°C to 800°C at the rate of 10°C/min using platinum crucible [34]. In TGA analysis, the weight loss in gram as well as percent loss for each step was recorded from the thermogram with respect to the

initial weight of the sample. Consequently, the DTG analysis revealed the thermogram from which, the onset, endset, peak temperature and integral area for each peak was recorded. The percent change in weight loss (W) was calculated using following equation 5:

$$\% \text{ change in weight loss} = \frac{[W_{\text{Treated}} - W_{\text{Control}}]}{W_{\text{Control}}} \times 100 \quad (5)$$

Where,  $W_{\text{Control}}$  and  $W_{\text{Treated}}$  are the weight loss of the control and the Biofield Energy Treated samples, respectively.

Also, the percent change in maximum thermal degradation temperature ( $T_{\text{max}}$ ) (M) was calculated using following equation 6:

$$\% \text{ change in } T_{\text{max}} \text{ (M)} = \frac{[M_{\text{Treated}} - M_{\text{Control}}]}{M_{\text{Control}}} \times 100 \quad (6)$$

Where,  $M_{\text{Control}}$  and  $M_{\text{Treated}}$  are the  $T_{\text{max}}$  values of the control and the Biofield Energy Treated pyridoxine hydrochloride samples, respectively.

**Differential Scanning calorimetry (DSC):** The DSC analysis of the samples was done under the dynamic nitrogen atmosphere with the help of DSC Q2000 differential scanning calorimeter, USA, at the flow rate of 50 mL/min. In this process, 2-4 mg sample was weighed and sealed in Aluminum pans. Later on, the sample was equilibrated at 30°C followed by heating up to 450°C at the rate of 10° C/min under nitrogen gas as purge atmosphere [34]. The thermogram reveals the value for onset, end set, peak temperature, peak height (mJ or mW), peak area, and change in heat (J/g) for each peak. Later on, the percent change in melting temperature (T) of

the control and the Biofield Energy Treated samples was calculated using following equation 7:

$$\% \text{ change in melting temperature} = \frac{[T_{\text{Treated}} - T_{\text{Control}}]}{T_{\text{Control}}} \times 100 \quad (7)$$

Where,  $T_{\text{Control}}$  and  $T_{\text{Treated}}$  are the melting temperature of the control and the Biofield Energy Treated pyridoxine hydrochloride samples, respectively.

Also, the percent change in the latent heat of fusion ( $\Delta H$ ) was calculated using following equation 8:

$$\% \text{ change in latent heat of fusion} = \frac{[\Delta H_{\text{Treated}} - \Delta H_{\text{Control}}]}{\Delta H_{\text{Control}}} \times 100 \quad (8)$$

Where,  $\Delta H_{\text{Control}}$  and  $\Delta H_{\text{Treated}}$  are the latent heat of fusion of the control and the Biofield Energy Treated pyridoxine hydrochloride, respectively.

## Results and Discussion

### Particle Size Analysis (PSA)

The particle size analysis was done for both the pyridoxine hydrochloride samples and the results are given in Table 1. The particle size distribution of the control pyridoxine hydrochloride was found at  $d_{10} = 9.22 \mu\text{m}$ ,  $d_{50} = 28.5 \mu\text{m}$ ,  $d_{90} = 92.3 \mu\text{m}$ , and  $D(4, 3) = 41.0 \mu\text{m}$ . Moreover, the particle size distribution of the Biofield Energy Treated sample was observed at  $d_{10} = 8.67 \mu\text{m}$ ,  $d_{50} = 28.3 \mu\text{m}$ ,  $d_{90} = 111.0 \mu\text{m}$ , and  $D(4, 3) = 46.8 \mu\text{m}$ . The analysis revealed that the particle size values at  $d_{10}$ ,  $d_{50}$ ,  $d_{90}$ , and  $D(4, 3)$  in the Biofield Energy Treated sample were significantly altered by -5.97%, -0.70%, 20.26%, and 14.15%, respectively compared to the control sample.

Test Item	$d_{10}$ ( $\mu\text{m}$ )	$d_{50}$ ( $\mu\text{m}$ )	$d_{90}$ ( $\mu\text{m}$ )	$D(4,3)$ ( $\mu\text{m}$ )	SSA( $\text{m}^2/\text{Kg}$ )
Control sample	9.22	28.5	92.3	41.0	283.0
Biofield Energy Treated sample	8.67	28.3	111.0	46.8	292.1
Percent change* (%)	-5.97	-0.70	20.26	14.15	3.22

**Table 1:** Particle size distribution of the control and the Biofield Energy Treated pyridoxine hydrochloride.

$d_{10}$ ,  $d_{50}$ , and  $d_{90}$ : particle diameter corresponding to 10%, 50% and 90% of the cumulative distribution,  $D(4,3)$ : the average mass-volume diameter, SSA: the specific surface area; \*denotes the percentage change in the particle size distribution of the Biofield Energy Treated sample with respect to the control sample.

Besides, the specific surface area of the Biofield Energy Treated pyridoxine hydrochloride (292.10  $\text{m}^2/\text{Kg}$ ) was

observed to be increased by 3.22% compared with the control sample (283.00  $\text{m}^2/\text{Kg}$ ). It is assumed that the Trivedi Effect® might act as an external force that resulted in the alteration of the particle sizes of pyridoxine hydrochloride along with its surface area. It was reported that a drug having increased surface area might show improved solubility, dissolution rate, and bioavailability profile [35,36]. Thus, it is anticipated that the Biofield Energy Treated sample might offer better bioavailability as compared to the untreated sample.

### Powder X-ray Diffraction (PXRD) Analysis

The PXRD diffractograms of the control and the Biofield Energy Treated pyridoxine hydrochloride samples are shown in Figure 1. The diffractograms of both the samples possess sharp and intense peaks thereby showing the crystalline nature of both the samples. Moreover, the PXRD data such

as Bragg angle ( $2\theta$ ), relative peak intensity (%), FWHM was collected from these diffractograms and were used further regarding the analysis of crystallite size ( $G$ ) for both the samples (Table 2). In this regard, the Scherer equation [37] was used for calculating the crystallite sizes of both the samples across various planes.

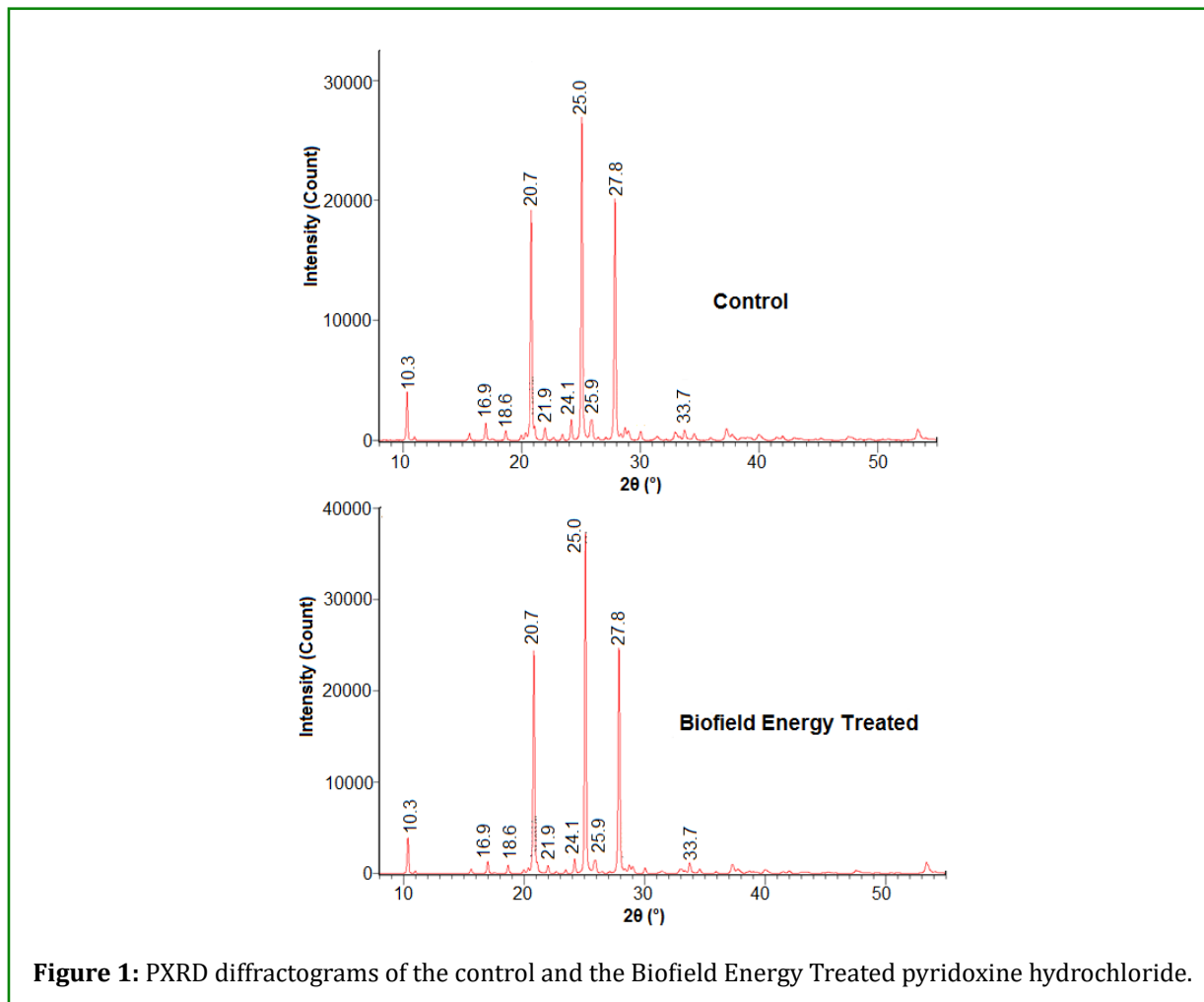


**Figure 1:** PXRD diffractograms of the control and the Biofield Energy Treated pyridoxine hydrochloride.

The highest peak intensity (100%) in the PXRD diffractograms of the control and the Biofield Energy Treated samples were observed at  $2\theta$  equal to  $25.0^\circ$  (Table 2, Entry 7). However, the relative intensities of the peaks at  $2\theta$  equal to  $10.3^\circ$ ,  $16.9^\circ$ ,  $18.6^\circ$ ,  $20.7^\circ$ ,  $21.9^\circ$ ,  $24.1^\circ$ ,  $25.9^\circ$ , and  $27.8^\circ$  (Table 2, entry 1-6, 8, and 9) in the Biofield Energy Treated sample were observed to be significantly reduced from 7.50% to 41.32% compared to the control sample. Besides, the relative intensity of the peak at  $33.7^\circ$  (Table 2, entry 10) in the Biofield Energy Treated sample remained same as that of the control sample. It showed that the crystallinity of the Biofield Energy Treated sample was reduced as compared to the control sample. On the other hand, the crystallite sizes of

the Biofield Energy Treated sample at  $2\theta$  equal to  $10.3^\circ$ ,  $21.9^\circ$ ,  $24.1^\circ$ ,  $25.9^\circ$ ,  $27.8^\circ$ , and  $33.7^\circ$  (Table 2, entry 1, 5, 6, and 8-10) were found to be significantly altered from -38.48% to 9.10% as compared to the control sample. However, the crystallite sizes of the Biofield Energy Treated sample at position  $2\theta$  equal to  $16.9^\circ$ ,  $18.6^\circ$ ,  $20.7^\circ$ , and  $25.0^\circ$  (Table 2, entry 2-4 and 7) remained same as that of the control sample. Also, the average crystallite size of the Biofield Energy Treated sample (31.60 nm) was significantly reduced by 6.23% than the control sample (33.70 nm). Thus, the analysis showed that the crystallinity as well as the crystallite size of the Biofield Energy Treated pyridoxine hydrochloride was significantly decreased when compared with the control sample.

Entry No.	Bragg angle( $2\theta$ )	Relative Intensity (%)			Crystallite size (G, nm)		
		Control	Treated	% Change*	Control	Treated	% Change*
1	10.3	14.97	10.48	-29.99	34.55	31.41	-9.10
2	16.90	5.17	3.53	-31.72	34.79	34.79	0.00
3	18.60	2.91	2.46	-15.46	31.70	31.70	0.00
4	20.70	70.96	65.64	-7.50	31.80	31.80	0.00
5	21.90	3.76	2.38	-36.70	43.83	26.96	-38.48
6	24.10	6.34	4.26	-32.81	29.32	31.99	9.10
7	25.00	100	100	0.00	32.05	32.05	0.00
8	25.90	6.05	3.55	-41.32	29.43	32.10	9.10
9	27.80	73.9	65.51	-11.35	29.54	27.27	-7.70
10	33.70	3.1	3.1	0.00	39.96	35.96	-10.01

**Table 2:** PXRD data for the control and the Biofield Energy Treated pyridoxine hydrochloride.

\*denotes the percentage change in the crystallite size of the Biofield Energy Treated sample with respect to the control sample.

It was previously reported that the Biofield Energy Treatment has a significant impact on the crystalline structure of compounds as it might produce a new polymorph by altering the relative intensities and crystallite sizes of the characteristic plane and thereby the crystal morphology [38,39]. Thus, it could be anticipated that the significant alterations in the crystallite size and relative intensities of the Biofield Energy Treated sample might indicate the alteration in its crystal morphology as compared to the control sample. Moreover, the reduced intensity of characteristic peaks and

crystallinity may be responsible for the increased dissolution rate of compound [35,40]. Thus, it could be concluded that the Biofield Energy Treated pyridoxine hydrochloride might offer better dissolution and bioavailability profile in its oral formulation as compared to the untreated sample.

#### Fourier Transform Infrared (FT-IR) Spectroscopy

The FT-IR spectra of the control and the Biofield Energy Treated pyridoxine hydrochloride are shown in Figure 2.

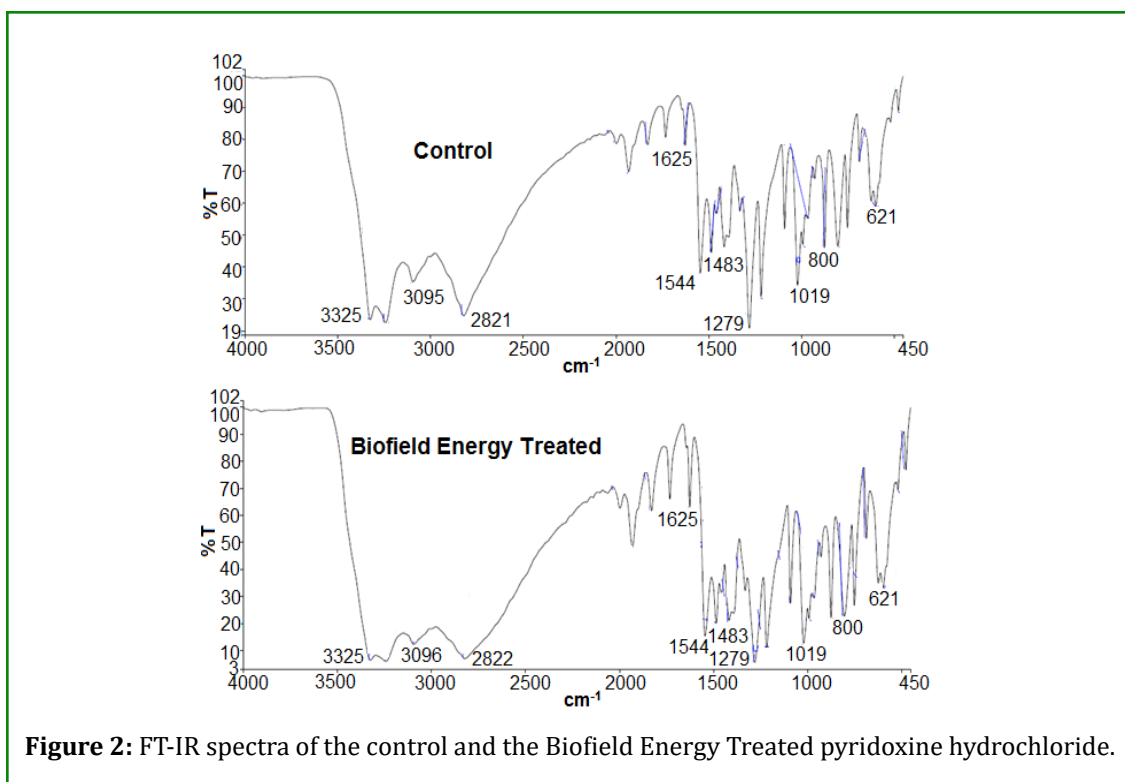


**Figure 2:** FT-IR spectra of the control and the Biofield Energy Treated pyridoxine hydrochloride.

The FT-IR spectra of both the pyridoxine hydrochloride showed the clear stretching and bending peaks in the functional group and fingerprint region. The broad peaks in the functional group area of the spectra of both the samples were observed near  $3325\text{ cm}^{-1}$  due to O-H stretching. The spectra showed aromatic C-H stretching at  $3095\text{ cm}^{-1}$  for both the samples. Also, the spectra showed aliphatic C-H stretching in the control sample at  $2821\text{ cm}^{-1}$  and  $2822\text{ cm}^{-1}$  in the Biofield Energy Treated sample. Moreover, both samples showed the aromatic C=N stretching peak at  $1625\text{ cm}^{-1}$ . Later on, the aromatic C=C stretching peaks were observed at  $1483$ , and  $1544\text{ cm}^{-1}$  in the spectra of control as well as the Biofield Energy Treated samples of pyridoxine hydrochloride [41]. The fingerprint region of both the samples, *i.e.*, the control and the Biofield Energy Treated sample remained same. It concluded that the FT-IR spectra of both the samples did not show any changes in the vibrational frequencies. Overall,

there was no alteration in the structural properties observed in the Biofield Energy Treated sample as compared to the control sample.

### Ultraviolet-visible Spectroscopy (UV-Vis) Analysis

The UV-vis spectra of both the samples are shown in Figure 3. The UV spectrum of the control sample showed the maximum absorbance at  $205\text{ nm}$  ( $\lambda_{\text{max}}$ ) and  $293\text{ nm}$  ( $\lambda_{\text{max}}$ ). The Biofield Energy Treated sample also showed similar peaks at  $205\text{ nm}$  and  $293\text{ nm}$ ; however, the peak at  $205\text{ nm}$  showed a minor shift of absorbance maxima from  $1.1396$  (in the control sample) to  $1.1430$  in the treated sample. Thus, the UV-Vis studies didn't show any difference in the control and the Biofield Energy Treated sample regarding  $\lambda_{\text{max}}$ , which revealed the similar molecular structure [42] of the Biofield Energy Treated sample as that of the control sample.

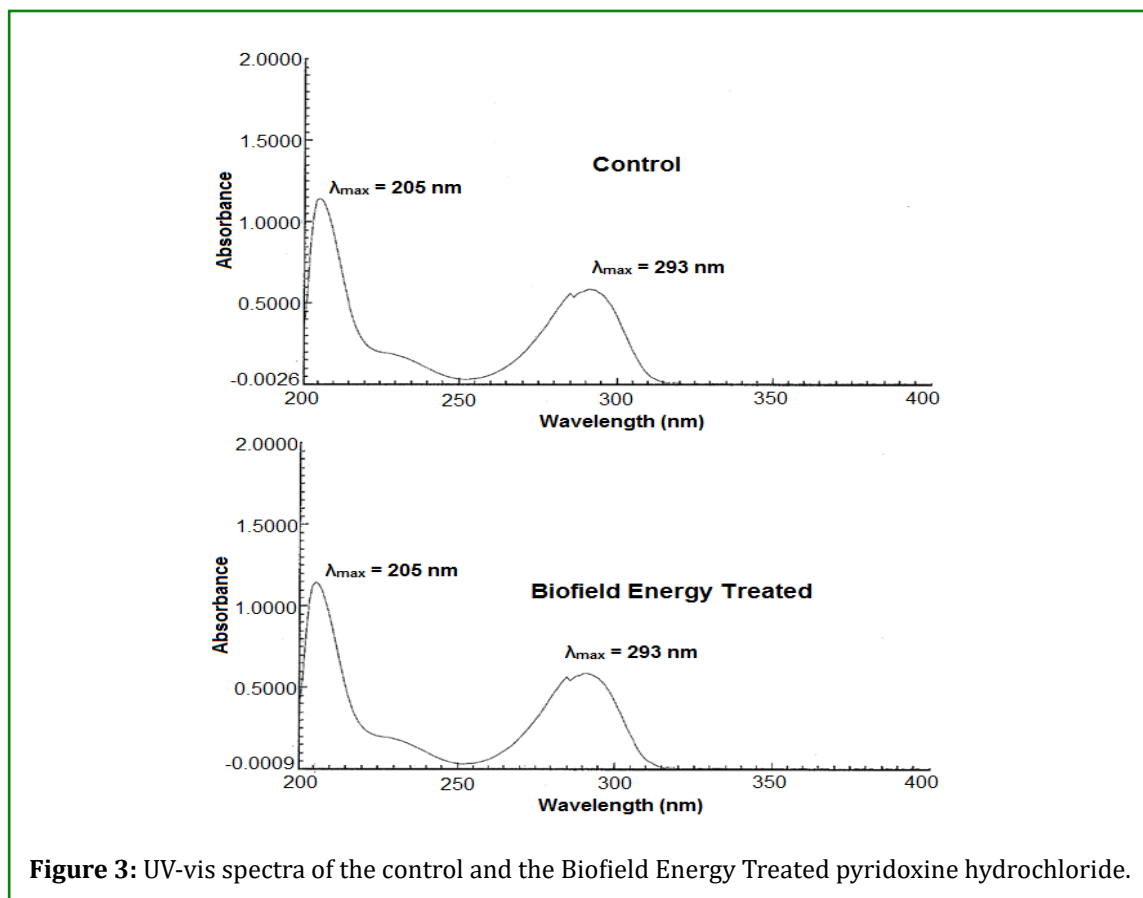


**Figure 3:** UV-vis spectra of the control and the Biofield Energy Treated pyridoxine hydrochloride.

### Thermal Gravimetric Analysis (TGA)/ Differential Thermogravimetric Analysis (DTG)

The TGA/DTG technique was used to study the thermal stability profile of the control and the Biofield Energy Treated pyridoxine hydrochloride. The TGA thermograms of both the samples showed three steps of thermal degradation

(Figure 4). According to previous studies, the pyridoxine hydrochloride was thermally stable below  $150^{\circ}\text{C}$  [43,44] and the thermograms of both the samples were found to be in concordance with the mentioned literature. The analysis showed that the Biofield Energy Treated pyridoxine hydrochloride showed a significant reduction in the weight loss in 1<sup>st</sup> and 3<sup>rd</sup> steps of degradation by 19.05 and 3.03%,

respectively. Although, there was a slight increase in the percentage weight loss in the 2<sup>nd</sup> step by 0.35%, however, the total weight loss in the Biofield Energy Treated pyridoxine hydrochloride was also decreased by 1.02% compared to the

control sample (Table 3). It showed that the thermal stability of the Biofield Energy Treated sample was significantly improved as compared to the control sample.

Sample	TGA Weight loss (%)				DTG T <sub>max</sub> (°C)
	1 <sup>st</sup> step	2 <sup>nd</sup> step	3 <sup>rd</sup> step	Total	
Control	0.126	19.94	12.19	32.26	215.24
Biofield Energy Treated	0.102	20.01	11.82	31.93	214.01
% change*	-19.05	0.35	-3.03	-1.02	-0.57

**Table 3:** Thermal degradation steps of the control and the Biofield Energy Treated pyridoxine hydrochloride.

T<sub>max</sub>: Maximum thermal degradation temperature, \*denotes the percentage change in the weight loss of the Biofield Energy Treated sample with respect to the control sample.

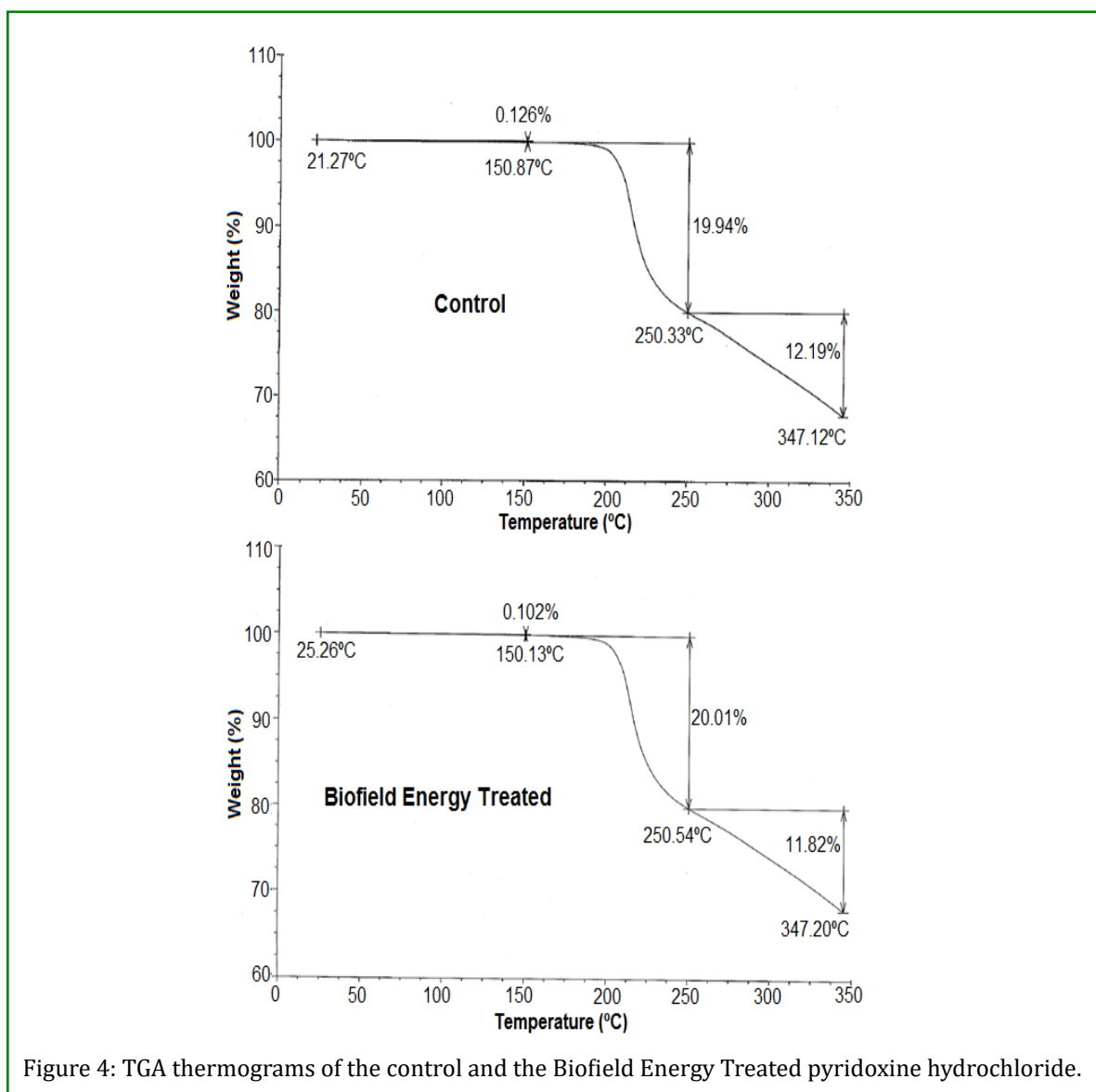
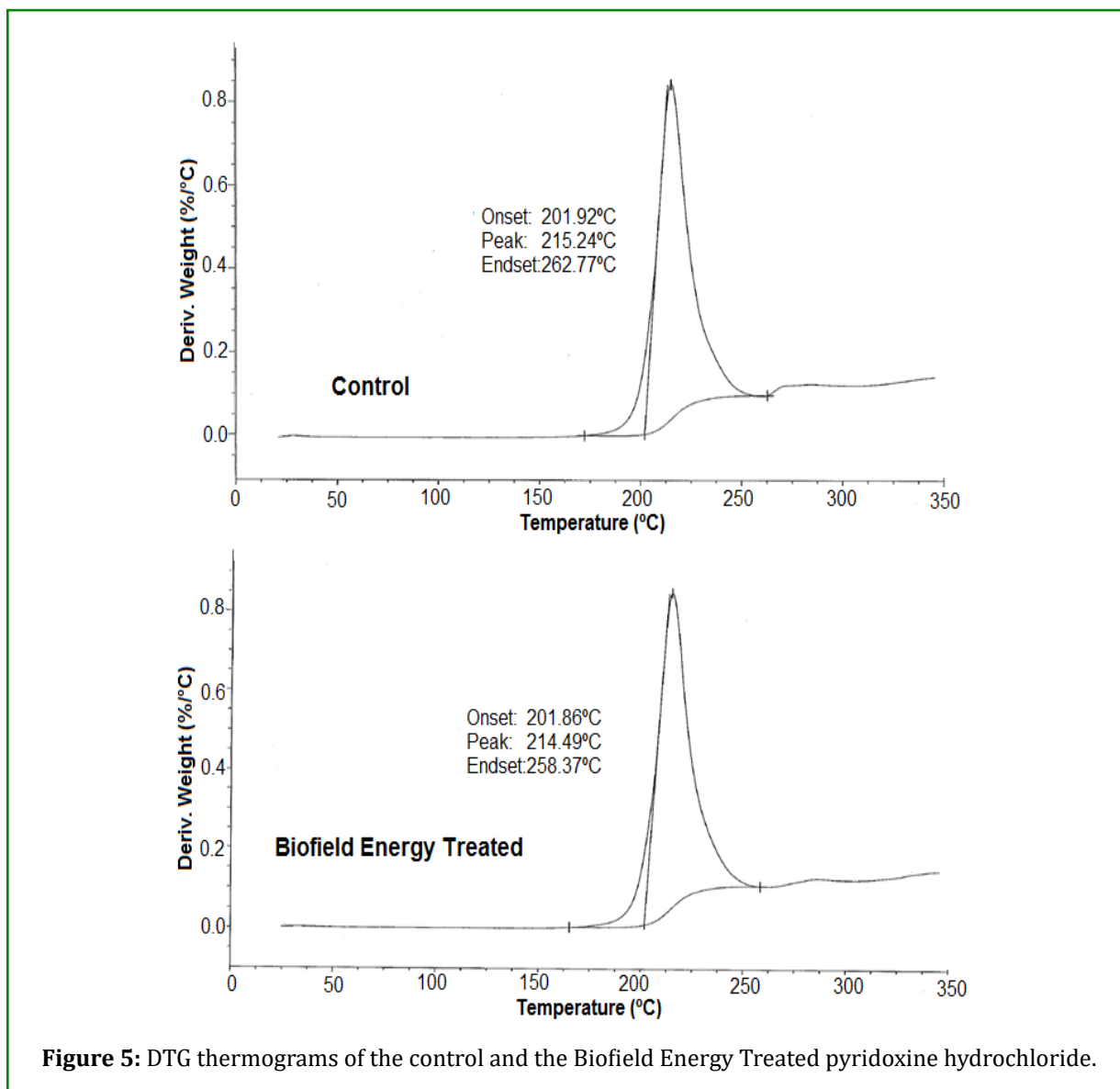


Figure 4: TGA thermograms of the control and the Biofield Energy Treated pyridoxine hydrochloride.

Besides, the DTG thermograms of both the samples (Figure 5) showed the single peak. Based on this, it was observed that the maximum degradation temperature ( $T_{max}$ ) of the Biofield Energy Treated sample (214.01°C) was slightly

decreased by 0.57% as compared to the control sample (215.24°C). Overall, the TGA/DTG studies revealed that the thermal stability of the Biofield Energy Treated sample was altered as compared with the control sample.



### Differential Scanning Calorimetry (DSC) Analysis

The thermal properties such as melting and crystallization properties of the pyridoxine hydrochloride sample were studied using the DSC technique [35]. The DSC thermograms of both the pyridoxine hydrochloride samples were shown in Figure 6. The thermograms of both the samples showed a single sharp endothermic peak (melting temperature), which was observed at 214.11°C in the control sample; whereas at 213.97°C in the Biofield Energy Treated sample. Thus, the

melting point of the Biofield Energy Treated sample was observed to be slightly decreased by 0.07% compared to the control sample (Table 4). Moreover, the latent heat of fusion ( $\Delta H$ ) of the Biofield Energy Treated sample was found to be 162.6J/g, which was significantly increased by 15.65% compared with the control sample (140.6J/g). It is assumed that the Biofield Energy treatment may cause alterations in the molecular chains as well as the crystallization structure of the pyridoxine hydrochloride [35], which might be responsible for the alteration in  $\Delta H$ .

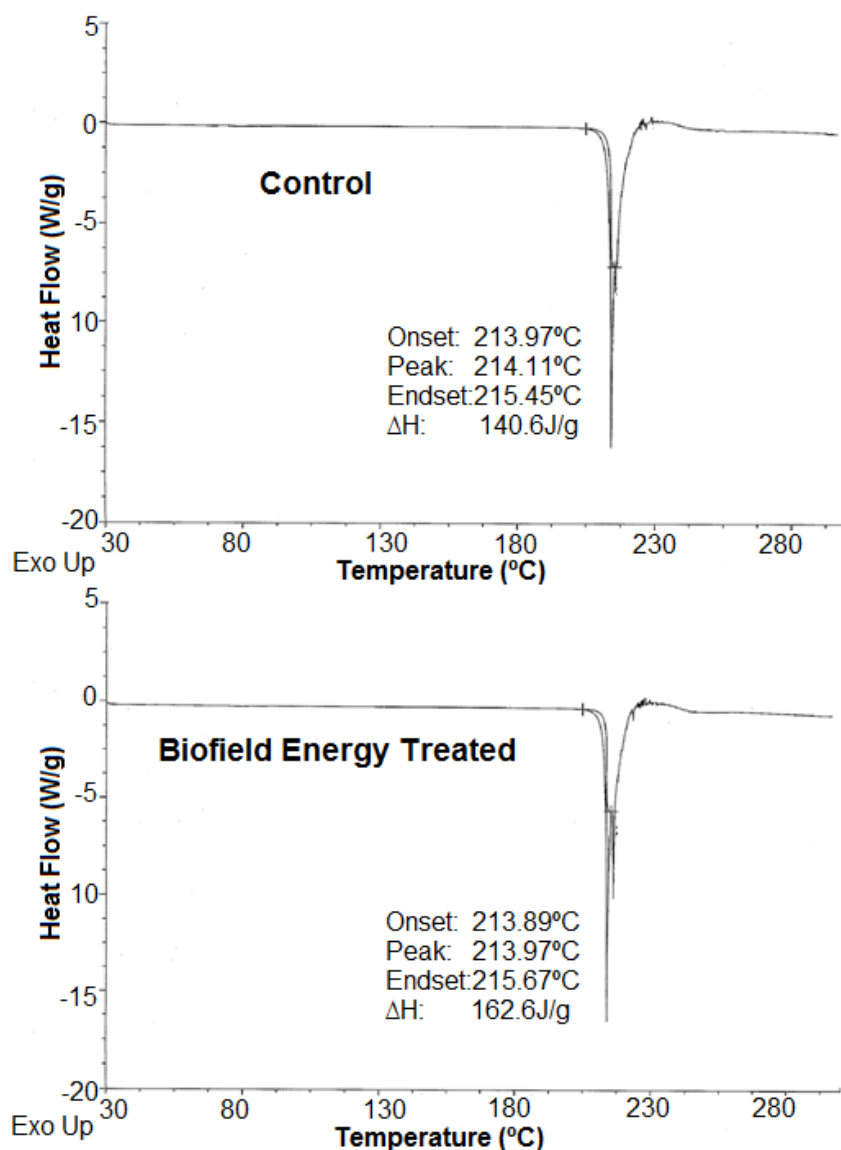


**Figure 6:** DSC thermograms of the control and the Biofield Energy Treated pyridoxine hydrochloride.

Sample	Melting Temperature (°C)			ΔH (J/g)
	T <sub>Onset</sub>	T <sub>Peak</sub>	T <sub>Endset</sub>	
Control	213.97	214.11	215.45	140.6
Biofield Energy Treated	213.89	213.97	215.67	162.6
% Change*	-0.04	-0.07	0.10	15.65

**Table 4:** Comparison of DSC data between the control and the Biofield Energy Treated pyridoxine hydrochloride.

T<sub>onset</sub>: Onset melting temperature, T<sub>peak</sub>: Peak melting temperature, T<sub>endset</sub>: Endset melting temperature, ΔH: Latent heat of fusion,

\*denotes the percentage change of the Biofield Energy Treated sample with respect to the control sample.

## Conclusion

The Trivedi Effect® - Energy of Consciousness Treatment has been found to possess a significant impact on the particle size, surface area, crystallite size, and relative intensities of the characteristic diffraction peaks and the thermal stability profile of pyridoxine hydrochloride. The particle size values at  $d_{10}$ ,  $d_{50}$ ,  $d_{90}$ , and  $D(4, 3)$  in the Biofield Energy Treated sample were significantly altered by -5.97%, -0.70%, 20.26%, and 14.15%, respectively compared with the control sample. Also, the specific surface area of the Biofield Energy Treated sample was significantly increased by 3.22% compared to the control sample. The PXRD studies revealed the reduction in the relative intensities of the most characteristic diffraction peaks from 7.50% to 41.32% in the Biofield Energy Treated sample compared with the control sample. Subsequently, the crystallite sizes corresponding to those diffraction peaks were also significantly altered from -38.48% to 9.10% in the Biofield Energy Treated sample compared with the control sample. Besides, the Biofield Energy Treated sample showed 6.23% reduction in the average crystallite size as compared with the control sample.

The thermal studies involving TGA analysis showed that the Biofield Energy Treated sample exhibited a significant reduction in the weight loss in 1<sup>st</sup> and 3<sup>rd</sup> steps of degradation by 19.05 and 3.03%, respectively; however, there was a slight increase of 0.35% in the 2<sup>nd</sup> step of degradation as compared to the control sample. Also, there was a reduction of 1.02% in the total weight loss of the Biofield Energy Treated pyridoxine hydrochloride as compared to the control sample. Besides, the DTG analysis indicated a slight reduction (0.57%) in the  $T_{max}$  of the Biofield Energy Treated sample compared with the control sample. Overall, the thermal analysis indicated the significant increase in the thermal stability of the Biofield Energy Treated pyridoxine hydrochloride than the control sample. DSC analysis of both the samples revealed a slight reduction in the melting point of the Biofield Energy Treated sample along with a significant increase in the latent heat of fusion by 15.65% compared to the control sample. Thus, it could be concluded that the Trivedi Effect® might help in producing a new polymorphic form of pyridoxine hydrochloride that would be more soluble, having a higher dissolution rate and bioavailability profile as compared to the untreated pyridoxine hydrochloride. Hence, the Biofield Energy Treated pyridoxine hydrochloride might show better therapeutic response against several disorders such as, pyridoxine deficiency, premenstrual syndrome, Alzheimer's disease, celiac disease, sideroblastic anemia, pyridoxine-dependant seizures, cardiovascular disease, metabolic disorders, autoimmune disorders, pulmonary tuberculosis, hyperhomocysteinemia, attention deficit hyperactivity disorder (ADHD), depression, dysmenorrhea, dermatitis with cheilosis, birth outcomes, carpal tunnel syndrome,

stroke recurrence, hyperkinetic cerebral dysfunction syndrome, immune system function, cognitive function, McArdle's disease, febrile seizures, autism, etc.

## Acknowledgement

The authors are grateful to GVK Biosciences Pvt. Ltd., Trivedi Science, Trivedi Global, Inc., and Trivedi Master Wellness for their assistance and support during this work.

## References

- McCormick D (2006) Vitamin B<sub>6</sub> in Present Knowledge in Nutrition. In: Bowman B, Russell R, (Eds.), International Life Sciences Institute, 9<sup>th</sup>(Edn.), Washington, DC.
- Mackey A, Davis S, Gregory J (2005) Vitamin B<sub>6</sub> in modern nutrition in health and disease. NIH.
- Simpson JL, Bailey LB, Pietrzik K, Shane B, Holzgreve W (2010) Micronutrients and women of reproductive potential: required dietary intake and consequences of dietary deficiency or excess. Part I-Folate, Vitamin B<sub>12</sub>, Vitamin B<sub>6</sub>. J Matern Fetal Neonatal Med 23(12): 1323-1343.
- Bailey RL, Gahche JJ, Lentino CV, Dwyer JT, Engel JS, et al. (2011) Dietary supplement use in the United States, 2003-2006. J Nutr 141(2): 261-266.
- Morris MS, Picciano MF, Jacques PF, Selhub J (2008) Plasma pyridoxal 5'-phosphate in the US population: the National Health and Nutrition Examination Survey, 2003-2004. Am J Clin Nutr 87(5): 1446-1454.
- Merrill AH, Henderson JM (1987) Diseases associated with defects in vitamin B<sub>6</sub> metabolism or utilization. Annu Rev Nutr 7: 137-156.
- Dakshinamurti S, Dakshinamurti K (2007) Vitamin B<sub>6</sub> in Handbook of Vitamins, In: Zempleni J, Rucker RB, McCormick DB, Suttie JW, (Eds.), 4<sup>th</sup>(Edn.), CRC Press, Taylor & Francis Group, Boca Raton, USA, pp: 315-360.
- Chiang EP, Bagley PJ, Selhub J, Nadeau M, Roubenoff R (2003) Abnormal vitamin B<sub>6</sub> status is associated with severity of symptoms in patients with rheumatoid arthritis. Am J Med 114(4): 283-287.
- Kashanian M, Mazinani R, Jalalmanesh S (2007) Pyridoxine (vitamin B<sub>6</sub>) therapy for premenstrual syndrome. Int J Gynaecol Obstet 96(1): 43-44.
- Albert CM, Cook NR, Gaziano JM, Zaharris E, MacFadyen J, et al. (2008) Effect of folic acid and B vitamins on risk of cardiovascular events and total mortality among women at high risk for cardiovascular disease: a randomized

- trial. JAMA 299(17): 2027-2036.
11. Trivedi MK, Mohan TRR (2016) Biofield energy signals, energy transmission and neutrinos. *Ameri J Mode Phy* 5(6): 172-176.
  12. Warber SL, Cornelio D, Straughn J, Kile G (2004) Biofield energy healing from the inside. *J Altern Complement Med* 10(6): 1107-1113.
  13. Hammerschlag R, Levin M, McCraty R, Bat N, Ives JA, et al. (2015) Biofield physiology: A framework for an emerging discipline. *Glob Adv Health Med* 4(S1): 35-41.
  14. Trivedi MK, Branton A, Trivedi D, Shettigar H, Bairwa K, et al. (2015) Fourier transform infrared and ultraviolet-visible spectroscopic characterization of biofield treated salicylic acid and sparfloxacin. *Nat Prod Chem Res* 3: 186.
  15. Trivedi MK, Patil S, Tallapragada RM (2013) Effect of biofield treatment on the physical and thermal characteristics of vanadium pentoxide powders. *J Material Sci Eng S* 11: 001.
  16. Trivedi MK, Branton A, Trivedi D, Nayak G, Mondal SC, et al. (2015) Evaluation of biochemical marker - glutathione and DNA fingerprinting of biofield energy treated *Oryza sativa*. *Ameri J BioSci* 3(6): 243-248.
  17. Trivedi MK, Branton A, Trivedi D, Nayak G, Gangwar M, et al. (2016) Molecular analysis of biofield treated eggplant and watermelon crops. *Adv Crop Sci Tech* 4(1): 208.
  18. Trivedi MK, Branton A, Trivedi D, Nayak G, Balmer AJ, et al. (2017) Evaluation of physicochemical, thermal, structural, and behavioral properties of magnesium gluconate treated with energy of consciousness (the Trivedi Effect®). *J Drug Design Medici Chemi* 3(1): 5-17.
  19. Trivedi MK, Branton A, Trivedi D, Nayak G, Balmer AJ, et al. (2017) Evaluation of physicochemical, spectral, thermal and behavioral properties of the biofield energy healing treated sodium selenate. *Sci J Chemi* 5(2): 12-22.
  20. Trivedi MK, Branton A, Trivedi D, Nayak G, Balmer AJ, et al. (2017) Study of the energy of consciousness healing treatment on physical, structural, thermal, and behavioral properties of zinc chloride. *Modern Chemi* 5(2): 19-28.
  21. Trivedi MK, Branton A, Trivedi D, Nayak G, Singh R, et al. (2015) Characterisation of physical, spectral and thermal properties of biofield treated resorcinol. *Organic Chem Curr Res* 4(3): 146.
  22. Trivedi MK, Patil S, Shettigar H, Singh R, Jana S (2015) An impact of biofield treatment on spectroscopic characterization of pharmaceutical compounds. *Mod Chem Appl* 3(3): 159.
  23. Trivedi MK, Branton A, Trivedi D, Nayak G, Bairwa K, et al. (2015) Spectroscopic characterization of disulfiram and nicotinic acid after biofield treatment. *J Anal Bioanal Tech* 6(5): 265.
  24. Trivedi MK, Branton A, Trivedi D, Nayak G, Bairwa K, et al. (2015) Physicochemical and spectroscopic characterization of biofield treated triphenyl phosphate. *Ameri J Applied Chemi* 3(5): 168-173.
  25. Trivedi MK, Branton A, Trivedi D, Nayak G, Bairwa K, et al. (2015) Physical, thermal, and spectroscopic characterization of biofield energy treated methyl-2-naphthyl ether. *J Environ Anal Chem* 2: 162.
  26. Trivedi MK, Branton A, Trivedi D, Nayak G, Bairwa K, et al. (2015) Physicochemical and spectroscopic characteristics of biofield treated p-chlorobenzophenone. *Ameri J Phy Chem* 4(6): 48-57.
  27. Trivedi MK, Nayak G, Patil S, Tallapragada RM, Latiyal O, et al. (2015) Impact of biofield treatment on atomic and structural characteristics of barium titanate powder. *Ind Eng Manage* 4(3): 166.
  28. Trivedi MK, Tallapragada RM, Branton A, Trivedi D, Nayak G, et al. (2015) Characterization of physical and structural properties of aluminum carbide powder: Impact of biofield treatment. *J Aeronaut Aerospace Eng* 4(1): 142.
  29. Trivedi MK, Branton A, Trivedi D, Nayak G, Mondal SC, et al. (2015) In vitro evaluation of biofield treatment on viral load against human immunodeficiency-1 and cytomegalo viruses. *Ameri J Health Res* 3(6): 338-343.
  30. Trivedi MK, Patil S, Shettigar H, Gangwar M, Jana S (2015) In vitro evaluation of biofield treatment on cancer biomarkers involved in endometrial and prostate cancer cell lines. *J Cancer Sci Ther* 7: 253-257.
  31. Trivedi MK, Branton A, Trivedi D, Nayak G, Mondal SC, et al. (2015) Evaluation of plant growth regulator, immunity and DNA fingerprinting of biofield energy treated mustard seeds (*Brassica juncea*). *Agri Fores Fisher* 4(6): 269-274.
  32. Trivedi MK, Branton A, Trivedi D, Nayak G, Mondal SC, et al. (2015) Evaluation of biochemical marker-glutathione and DNA fingerprinting of biofield energy treated *Oryza sativa*. *Ameri J BioSci* 3(6): 243-248.
  33. Trivedi MK, Branton A, Trivedi D, Nayak G, Lee AC, et al. (2017) A comprehensive analytical evaluation of

- the Trivedi Effect® - Energy of Consciousness Healing Treatment on the physical, structural, and thermal properties of zinc chloride. *Ameri J Applied Chem* 5(1): 7-18.
34. Trivedi MK, Branton A, Trivedi D, Nayak G, Plikerd WD, et al. (2017) A systematic study of the biofield energy healing treatment on physicochemical, thermal, structural, and behavioral properties of Magnesium Gluconate. *Int J Bioorganic Chem* 2(3): 135-145.
35. Zhao Z, Xie M, Li Y, Chen A, Li G, et al. (2015) Formation of curcumin nanoparticles *via* solution enhanced dispersion by supercritical CO<sub>2</sub>. *Int J Nanomedicine* 10: 3171-3181.
36. Mosharrof M, Nystrom C (1995) The effect of particle size and shape on the surface specific dissolution rate of micro-sized practically insoluble drugs. *Int J Pharm* 122(1-2): 35- 47.
37. Langford JI, Wilson AJC (1978) Scherrer after sixty years: A survey and some new results in the determination of crystallite size. *J Appl Cryst* 11: 102-113.
38. Trivedi MK, Branton A, Trivedi D, Nayak G, Plikerd WD, et al. (2017) Evaluation of the physicochemical, spectral, thermal and behavioral properties of sodium selenate: influence of the energy of consciousness healing treatment. *Ameri J Quantum Chemi Molecul Spectroscop* 2(2): 18-27.
39. Trivedi MK, Branton A, Trivedi D, Nayak G, Lee AC, et al. (2017) Evaluation of the impact of biofield energy healing treatment (the Trivedi Effect®) on the physicochemical, thermal, structural, and behavioural properties of magnesium gluconate. *Int J Nutri Food Sci* 6(2): 71-82.
40. Raza K, Kumar P, Ratan S, Malik R, Arora S (2014) Polymorphism: The phenomenon affecting the performance of drugs. *SOJ Pharm Pharm Sci* 1(2): 10.
41. Stuart BH (2004) Infrared spectroscopy: Fundamentals and applications. In: John Wiley & Sons (Eds.), analytical techniques in the sciences, Ltd., Chichester, UK.
42. Hesse M, Meier H, Zeeh B (1997) Spectroscopic methods in organic chemistry, Georg Thieme Verlag Stuttgart, New York. *J Plant Physiology* 151(6): 768.
43. Branton A, Jana S (2017) Evaluation of the Effect of the Energy of Consciousness Healing Treatment on Physicochemical and Thermal Properties of Pyridoxine Hydrochloride. *Ameri J Phys Chem* 6(4): 49-58.
44. Juhasz M, Kitahara Y, Takahashi S, Fujii T (2012) Study of the thermal stability properties of pyridoxine using thermogravimetric analysis. *J Analytical Letters* 45(11): 1519-1525.